Submitted version: February 25, 2003

Activity and Kinematics of members of the TW Hydrae Association [1]

I. Neill Reid

Space Telescope Science Institute, 3700 San Martin Drive, Baltimore, MD 21218

inr@stsci.edu

ABSTRACT

We present high-resolution echelle spectroscopy of twenty stars in 16 systems catalogued as members of the TW Hydrae association, and 16 stars identified as possible new members. We have calibrated the range of coronal and chromospheric activity expected for such young stars as a function of spectral type by combining our observations with literature data for field and open cluster stars. We also compute space motions for TWA members and candidate members with proper motion measurements, using two techniques to estimate distances to stars lacking direct trigonometric parallax measurements. The mean space motion of the four TWA members with known parallaxes is (U,V,W:-10.0,-17.8,-4.6)km s^{-1} . Fourteen of the candidates have properties inconsistent with cluster membership; the remaining two are potential new members, although further observations are required to confirm this possibility.

Subject headings: Galaxy: solar neighbourhood, (Galaxy:) open clusters and associations: individual (TW Hydrae)

1. Introduction

The TW Hydrae Association is a loose aggregate of 15 to 20 stellar systems with ages of 10 to 15 Myrs, lying at distances of only ≈60 parsecs from the Sun. The archetype, TW Hydrae, was identified as a T Tauri star by Herbig (1978). Unlike most T Tauris, TW Hydrae

[1]Based partly on observations made at the Keck Observatory which is operated by the Californian Association for Research in Astronomy, and was made possible by generous grants from the W. M. Keck Foundation.

is not associated with a parent molecular cloud, but the presence of a substantial gas- and dust-rich circumstellar disk, imaged at near-infrared wavelengths through both NICMOS (Krist *et al.*, 2000; Weinberger *et al.*, 2002) and ground-based (Trilling *et al.*, 2001) observations, clearly confirms its young age. Several other isolated T Tauri stars were identified within the same region by de la Reza *et al.*(1989) and Gregorio-Hetem *et al.*(1992). Kastner *et al.*(1997) proposed that the similar properties exhibited by these systems, particularly at X-ray wavelengths, indicated a physical association. Following up on the latter proposal, Webb *et al.*(1999 - WZP99) combined ROSAT data with photographic astrometry and low-resolution spectroscopy to identify seven additional T Tauri stars in five systems within a 200 square degree region centred on the putative cluster. Further observations by Sterzik *et al.*(1999 - SACP99), Webb (1999- W99) and Zuckerman *et al.*(2001 - ZWSB) have expanded the sample to include as many as 32 stars and brown dwarfs in twenty-one systems.

While it is clear that all of the stars in the TW Hydrae association have similar ages, it has not yet been established whether they all originated within the same star formation region. In particular, Jensen *et al.*(1998) have argued that backtracking 10 Myrs using the measured proper motions for TW Hya, HD 98800 and CD -36^{o}7429 does not place those stars in sufficient proximity for membership of the same star-forming cloud. Accurate distance estimates and full (U, V, W) space motions are required to test whether distributed or single-origin star formation provides a better model for the association as a whole, and it is partly to that end that we have obtained echelle observations of other candidate members.

High resolution spectroscopy can also be used to address another issue - multiplicity. The proximity and consequent bright apparent magnitudes of the TW Hydrae association stars provides a unique opportunity to examine the relative frequency of formation of single and multiple systems in a low-density star-forming system. It is clear even from the statistical summary given above that the TW Hydrae stars include a substantial number of binary and multiple systems. Most of the known companions have been identified through direct imaging and lie at separations exceeding 10 AU. Spectroscopy samples a different régime, and can reveal systems at much smaller separations of only a few stellar radii.

Our paper is organised as follows: Section 2 presents new spectroscopic and astrometric observations of both previously identified TWA members and new candidates. Section 3 considers the spectral characteristics, particularly the emission line activity, of the latter objects. Section 4 considers the space motions and identifies possible new members of TW Hydrae Association. Finally, Section 5 presents our conclusions.

2. Observations

2.1. The sample

The stars observed in this program include 18 previously-identified TW Hydrae association members, two of which (TWA 2AB and 3AB) are known to be unresolved ($< 1''$ separation) binaries, and 16 new candidate members. All of the latter were selected as candidate members (W99) based on their having relatively high X-ray fluxes, consistent with the activity expected in extremely young stellar systems. Several are included as likely members of the Lower Centaurus-Crux (LCC) Association in Mamajek, Meyer & Liebert's (2002) survey of post-T Tauri stars.

Since our obtaining those observations, a number of additional candidates have been proposed based on proper motion characteristics coupled with X-ray activity (Makarov & Fabricius, 2001 - MF01), and on spectral characteristics suggestive of low gravity and significant chromospheric activity (Gizis, 2002 - G02). Song *et al.*(2002) have discussed the spectral properties of the former sample, and show that only three stars have Hα and Li 6708Å line-strengths consistent with ages of 10 to 30 Myrs. Those three stars are probably members of the more distant LCC Association, but we include them in the present analysis for comparative purposes.

Table 1 collects photometry and positions for both the previously-identified TW Hydrae members, and for the new candidates considered in this paper. The naming conventions are from W99. One of the ROSAT sources, XACT 164, has three possible optical counterparts, labelled A, B and C in Figure 1. As discussed further below, the brightest optical candidate, star A, is clearly not related to the X-ray source.

Many of the stars listed in Table 1, particularly the new candidates, have relatively sparse photometric observations, but almost all have spectral type information. We have therefore used mean spectral-type/colour relations to estimate (B-V) and (V-I) colours (and hence bolometric corrections) and (V-R) colours (hence Hα continuum fluxes) where such data are lacking. Fitzgerald (1970) lists (B-V) colours as a function of spectral type, while Ducati *et al.*(2001) provide similar data for the Johnson RI system. We have used the equations given by Bessell (1979) to transform the latter to the Cousins system, and Figure 2 compares the mean relations against observational data for stars within 8-parsecs of the Sun (from Reid & Gizis, 1997). The Ducati *et al.*relations provide a reasonable match at earlier spectral types, but tend to underestimate the colours for mid-G and later dwarfs. We therefore adopt the median value from the nearby-star dataset as the appropriate colour for spectral types later than G5. A self-consistent set of optical photometry of all of these systems would clearly be useful.

2.2. Echelle spectroscopy

The majority of the stars listed in Table 1 were observed with the HIRES spectrograph (Vogt *et al.*, 1994) on the Keck-I 10-metre telescope. Most observations were made using the blue cross-disperser and collimator, covering the wavelength range 3770 to 5280Å with minimal gaps between orders. The setup is identical to that described by Zuckerman & Reid (1998), save that the B2 slit ($0''57$) was used, giving a resolution of 68,000 or 4.4 kms^{-1}. These spectra were obtained on the nights of June 23 and 24 1998 and April 19 and 20 1999 (UT dates). The remaining stars were observed on December 29 and 30 1999 (UT), using the red cross-disperser and collimator. Those observations cover the wavelength range 6200 to 8500Å and match those described by Reid & Mahoney (2000 - RM2000). We used the C1 slit ($0''86$) to give a resolution of 45,000 or 6.67 kms^{-1}.

All of the observations were reduced and analysed using the same combination of procedures described by RM2000. The *mckee* suite of programs written by T. Barlow was used to extract the echelle orders, subtracting the bias level and sky background as well as dividing the data by tungsten flat-field images. The extracted spectra were wavelength calibrated using standard iraf routines, with the calibration defined by a single Th-Ar image taken at the start of each series of observations. As discussed in RM2000, tests show that the wavelength calibration of HIRES is stable to 2 kms^{-1} over the course of a full night's observations. Stability should be higher for the present datasets, since all of the targets are bright, with integration times of less than 300 seconds, and each set of observations took less than 90 minutes.

We also obtained observations of several early-type M dwarfs as radial velocity standards. Gliese 507.1 (M1.5), Gl 526 (M1.5) and Gl 638 (K5) were observed in June 1998; Gl 526 in April 1999; and Gl 447 (M4) in December 1999. The spectral types are taken from Reid, Hawley & Gizis (1995a). All of these stars have accurate radial velocity determinations by Marcy & Benitz (1989), and the spectral types are reasonably matched to the majority of the TW Hydrae members. We have used these stars as cross-correlation templates in the *iraf* routine *fxcor* to determine radial velocities for the later-type stars in the present sample. In the case of earlier-type stars, such as HD 110817 and HD 102458, the radial velocities are determined directly from the measured wavelength of the Ca II K line. The apparent radial velocities are adjusted to heliocentric values using corrections derived from the iraf routine *rvcorrect*. We estimate that these results are accurate to better than ± 2 kms^{-1}, while the cross-correlation measurements are accurate to 1 to 1.5 kms^{-1} for narrow-lined spectra. In support of this assertion, our results agree to better than 1 kms^{-1} with recent observations of several TWA members by Torres *et al.*(2003). The derived radial velocities are listed in Tables 2 and 3.

Most of the stars exhibit significant emission from the hydrogen Balmer series and the Ca II H & K lines. Equivalent widths for Hα, Hβ, Hγ and the Ca II K line are listed in Table 2, where we have supplemented our HIRES data with lower-resolution measurements from W99. Typical uncertainties are 0.1 to 0.25Å, set primarily by uncertainties in defining the continuum level. Moreover, these emission lines are likely to be time variable by up to 30%. TWA 6 was observed on three occasions, and there are clear variations in line strength; for example, the Hβ equivalent widths vary from 3.3Å (24/6/98) to 2.45Å (19/4/99).

A number of the stars have significant rotational velocities. We have estimated $v \sin i$ using the method outlined in RM2000: calibrating the width of the cross-correlation peak as a function of $v \sin i$. Taking Gl 526 ($v \sin i =< 2.9$ kms^{-1}; Delfosse *et al.*, 1998) and Gl 447 ($v \sin i =< 2$ kms^{-1}; Delfosse *et al.*, 1998) as templates, we selected 3 orders with no emission features and few strong atomic lines, and applied rotational broadening using the line-profile prescription given by Gray (1982). The broadened spectra were cross-correlated against the original data, using *fxcor* in *iraf*, and the width of the cross-correlation peak recorded. Experience has shown that this technique is reliable for low and moderate rotational velocities, $v \sin i < 30$ kms^{-1}, giving results which agree to within 3 kms^{-1} with independent measurements (Reid *et al.*, 2002). The uncertainties are larger at higher rotation rates, reaching 5 to 10 kms^{-1} at $v \sin i > 50$ kms^{-1}. However, at those velocities the absolute value of the rotation is less significant than simply identifying the star as a rapid rotator.

Rotational velocity estimates for all candidate TWA members are listed in Table 2. Several stars have very rapid rotational velocities, as expected for ages of less than 100 Myrs. Torres *et al.*(2003) have measured $v \sin i$ for four stars in our sample: TW Hydrae, Hen 600A (TWA 3A), -33:7795A (TWA 5A) and -36:7429A (TWA 9A). The agreement is reasonable, with our $v \sin i$ tending to be lower than the Torres *et al.*values by 2-3 kms^{-1}. The exception is Hen 600A, where Torres *et al.*measure $v \sin i = 20$ kms^{-1}, while our spectrum shows a sharp cross-correlation profile and narrow lines. The origin of this discrepancy is not clear.

2.3. Spectroscopic binaries

The TW Hydrae association includes a high fraction of binary and multiple systems. Using some of the observations discussed in this paper, three stars in Table 1, Hen 600A, TWA 5A and TWA 6 were reported as possible spectroscopic binaries by Webb *et al.*(1999). High-resolution spectroscopy by Muzerolle *et al.*(2000) confirms that the first mentioned star is double-lined, with a velocity difference of >40 km s^{-1} . In contrast, more detailed analysis of repeated observations of the last-mentioned star, TWA 6, indicates that the initial suggestion of binarity is probably incorrect. It seems likely that the anomalous cross-correlation profiles, which prompted that suggestion, stem from effects introduced by the relatively high rotational velocity.

The evidence in favour of binarity of the remaining star, TWA 5A, is given by the morphology of cross-correlation spectra derived by matching data for that star against our observations of TWA 10. The latter star has narrow lines, with no indication of binarity, and was also used as a template by Muzerolle *et al.*. The cross correlation peak is clearly double, with the bluer component slightly stronger and offset by 30 km s^{-1} from the redder component. The radial velocity listed in Table 2 is the average of the two values. None of the other stars in the present sample, either known members or new candidates, show evidence for binarity. With the addition of TWA 5Aab, the TW Hydrae system now includes at least one quadruple (HD 98800), two triple systems (TWA 5, Hen 600), seven binaries and eleven single stars.

3. Activity, radial velocities and TWA membership

Chromospheric and coronal activity are known to be age-dependent phenomena, both declining with increasing age for main-sequence stars. While the original models of coronal activity assumed acoustic heating (e.g. Ulmschneider, 1967), both phenomena are now regarded as manifestations of the stellar magnetic field. Chromospherically active stars exhibit emission in the alkaline lines (Ca, Na, K) and the Balmer series, while coronal activity is evident at X-ray wavelengths. Thus, an effective means of searching for young, nearby stars is correlating X-ray and optical imaging data, and identifying sources with potentially high activity. Positional accuracy can be an issue with X-ray survey data, leading to potential misidentification between bright stars and background X-ray sources, but direct spectroscopy can confirm whether the observed chromospheric activity is consistent with expectations.

The majority of candidate TW Hydrae members have been identified from ROSAT data. In this section, we compare the derived activity levels against measurements of field stars and cluster members, and consider whether the results are consistent with expectations for young stars. In addition, as described below, we use our radial velocity measurements as a check that the space motions are consistent with the known TWA members.

3.1. Radial velocities for TWA members

The members of a young stellar association are expected to have nearly identical space motions. As a consequence, the individual proper motions should be aligned, allowing the determination of a convergent point. The expected radial velocity, V_{pred}, for a cluster member is simply

$$V_{pred.} \;=\; V_S \cos \lambda_i$$

where V_S is the total space motion and λ_i the angular distance from the convergent point.

Makarov & Fabricius (MF01) have undertaken a convergent point analysis of the TW Hydrae Association. They find that the standard analysis yields a convergent point at $(\alpha = 5^h 23^m, \delta = -19^o 57')$, but predicts radial velocities in the range +3.2 to +5.8 km s^{-1} as opposed to the observed +10 to +13 km s^{-1} . MF01 suggest that the observed discrepancies stem from a superimposed expansion of cluster members. Their model places the association centroid at a distance of 73 pc. from the Sun and at $(\alpha = 11^h 1.6^m, \delta = -32^o 6')$, $\sim$ 16pc. beyond TW Hydrae, with an expansion term of 0.12 km s^{-1} pc^{-1} (where the distance is measured from the cluster centroid). Based on this model, MF01 identify 23 new candidate members, including the last three stars listed in Table 2. As discussed in §2.1, however, Song *et al.*(2002) find that few of these stars have the characteristics expected for an age of 10 Myrs. Thus, it remains unclear whether the expansion term introduced by MF01 has any validity.

For our present purposes, we have adopted a simpler, empirical approach. We assume that the direction of the convergent point derived by MF01 is valid, that TW Hydrae (V_S=22.1km s^{-1}) marks the cluster centroid, and adjust the angular separation to match the predicted and observed radial velocities for that star. The last step requires an angular separation of 55.5^o, rather than the 74.4^o derived by MF01, and places the convergent point at $(\alpha = 6^h 37^m, \delta = -28.6^o)$. The resultant values of $V_{pred.}$ are listed in Table 2. The predicted and observed velocities of previously-identified TW Hydrae members agree to within 2-3 km s^{-1} . The comparison suggests that this *ad hoc* technique allows us to weed out candidates with highly discrepant ($\Delta V >$ 6km s^{-1}) radial velocities.

3.2. Activity as a function of spectral type in main-sequence stars

The original demonstration of the age-activity correlation rests on observations of Ca II H&K emission by Wilson (1966) and Kraft (1967), codified by Skumanich (1972) as a $\tau^{-\frac{1}{2}}$ relation, where τ is age. Soderblom *et al.*(1991) have since shown that the underlying relation is more complex. Nonetheless, Skumanich showed that a broadly similar correlation holds for age and rotation for upper main-sequence (AFGK) stars, while observations with the Einstein satellite showed qualitatively similar behaviour at X-ray wavelengths (Vaiana *et al.*, 1981).

This behaviour is generally consistent with a model where magnetic activity is generated by an $\alpha\Omega$ dynamo (Parker, 1955), driven by shear between the inner radiative core and the outer convective envelope. The level of activity generally increases with decreasing mass along the main sequence. Theoretical stellar models predict that stars should become fully convective at effective temperatures of ≈3000K, corresponding to spectral type ≈M3/M4. At that point, the absence of a radiative core should eliminate the $\alpha\Omega$ dynamo. Thus, expectations were that magnetic activity should decline significantly for mid- and late-type M dwarfs. As is now well known, such is not the case. Nearby M dwarfs have substantial X-ray fluxes, detectable even by Einstein (Vaiana *et al.*, 1981), while extensive spectroscopic surveys have shown that chromospheric activity, as measured by Balmer emission, is approximately constant to spectral type M7 (Hawley *et al.*, 1996), declining only at later types (Gizis *et al.*, 2000). It seems likely that activity is generated by a turbulent dynamo mechanism in these fully-convective, later-type dwarfs (Hawley *et al.*, 1999).

Coronal activity is typically measured using the ratio between the observed X-ray flux and the total bolometric flux, $\frac{f_X}{f_{bol}}$. We have used an analogous relation to characterise chromospheric activity, $\frac{f_\alpha}{f_{bol}}$, where f_α is the observed flux in the Hα emission line (Reid *et al.*, 1995b). In our previous analyses, centred on K and M dwarfs, all of the targets have known distances, allowing the use of absolute bolometric magnitude as a surrogate for mass. That is not possible in the present study. However, spectral type serves as a ready alternative. We have therefore compiled literature data on chromospheric and coronal activity to provide a broader context for assessing measurements of the candidate TWA members.

Figure 3 plots coronal activity as a function of spectral type for nearby field stars, members of the Hyades and Pleiades clusters and the TW Hydrae Association stars. The field star X-ray data are taken from Huensch *et al.*(1999), with the spectral types taken from either the PMSU survey (Reid *et al.*, 1995a) or the preliminary CNS3 catalogue (Gliese & Jahreiss, 1991). The Hyades X-ray data are from Stern *et al.*(1981) for upper main-sequence stars and Reid *et al.*(1995b) and references therein for K and M dwarfs; the Pleiades data are from Micela *et al.*(1999) and Stauffer *et al.*(1994). Spectral types for the cluster stars are derived by combining either (B-V) or (V-I) colours with the relations discussed in §2.1. Data for the TW Hyd Association members are taken from WZP99, SACP99 and ZWSB. Most of the X-ray data for the new candidates are from W99 while the spectral types are taken from SIMBAD or derived from either (B-V) colours or our spectra.

Figure 4 plots chromospheric activity. The uppermost panel plots the Hα relative fluxes, where data are taken from the PMSU survey for field stars, from Reid *et al.*(1995b) for Hyades and Pleiades stars, and from the sources listed above for TWA members and candidate members. Since Hα emission is largely restricted to mid-K and later-type stars, we also show our measurements of equivalent widths of the Ca II K-line and Hβ for TWA members and candidates.

Both Figures 3 and 4 show a general progression of increasing activity with decreasing age at a given spectral type. The Pleiades stars are typically more active than the Hyades stars, which in turn lie along the upper edge of the field star distribution. Both cluster sequences show significant dispersion in activity at a given spectral type. The known TWA members are clearly significantly more active, both chromospherically and coronally, than the $\sim$ 120-Myr Pleiades stars, and provide a clear reference for potential new members, as discussed further in the following section.

3.3. TWA membership

Section §3.1 and 3.2 and Figures 3 and 4 provide the baseline data which permit a preliminary assessment of membership probability for TWA candidates. In this section, we measure each of the stars listed in Table 1 against that baseline.

TWA 19 Originally selected by W99 based on the high X-ray flux of the G-type primary, the presence of lithium absorption and significant chromospheric emission clearly indicates a young system. The Hipparcos parallax, however, places the system at a distance of over 100 parsecs, well beyond the four TWA members with trigonometric parallax data, and Song *et al.*(2002) suggest that the binary may be a member of the more distant ($\sim$ 130 pc.) Lower Centaurus Crux system.

XACT 164 (also listed as c99a* in W99) As noted above, there are three candidates for the optical counterpart for this ROSAT source. The brightest, star A in Figure 1, can be ruled out since it shows no Ca II emission. XACT 164 B is an early-type K dwarf with significant Ca II emission, while XACT 164 C is a chromospherically-active M dwarf with both Ca II and Hα emission. The $\frac{f_X}{f_{bol}}$ values listed in Table 2 are both derived from the same ROSAT flux measurement; either star could have an activity level consistent with an age of 10 Myrs. However, the Ca II emission lines in XACT 164 C are significantly weaker than in the early-type M dwarf TWA 2, while XACT 164 B is not only chromospherically active, but also a rapid rotator. Thus, XACT 164 B is a more likely candidate for the X-ray source, but its radial velocity is inconsistent with the value expected for a member of the TW Hydrae association. We exclude all three as likely TWA members.

HD 110817 This early-type K dwarf has moderate Ca II emission and relatively rapid rotation, although both properties may be less extreme than expected for an age of 10 Myrs. The radial velocity is (barely) consistent with TWA membership, although Mamajek *et al.* (2002) link HD 110817 with the LCC Association, with a high probability of membership (94-99%). We consider this star further below.

HD 112227 This G dwarf has moderate Ca II emission, significant rotation and coronal activity consistent with TWA membership. The observed radial velocity, however, disagrees by $\sim$ 6km s^{-1} with our predicted value. This is clearly a relatively young star, but, like TWA 19, it may be a member of the LCC Association, rather than TWA (see Mamajek *et al.*). We consider HD 112227 further in the following section.

HD 107434 This F6 dwarf was suggested as a common proper motion companion of HR 4796 by Jura *et al.* (1998). There is little Ca II emission, the star is not detected in the ROSAT survey and the negative radial velocity rules out membership of the TW Hydrae association.

HD 114335 As with HD 107434, Jura *et al.* (1998) identified this star as a possible cpm companion of HR 4796. There is no Ca II emission, the star is not detected in the ROSAT survey and the radial velocity differs by $\sim$ 7km s^{-1} from the value predicted by our convergent point model. We therefore exclude this star from TWA membership.

XACT 10 (also listed as c99a1 in W99) A chromospherically-active early-type K dwarf with relatively low rotation. The X-ray flux (assuming correct identification) indicates coronal activity consistent with the known TWA members. Webb finds no Hα emission, but measures an equivalent width of 0.22Å for the Li I 6708Å line (W99). We consider this star further below.

XACT 61 (also listed as c99a5 in W99) Similar in spectral type to the preceding star, the x-ray flux indicates a lower level of coronal activity, but still significantly above Pleiades stars of similar spectral type. The $v \sin i$ measurement indicates moderate rotation and the radial velocity is consistent with TWA membership. There is no emission at Hα and relatively weak (0.13 Å) lithium absorption (W99).

XACT 136 (also listed as c99a6 in W99) Another active K dwarf, the coronal activity matches that of XACT 61. The lower equivalent width measured for the Ca II line may be affected by the substantial rotational velocity. Given the significant broadening, the radial velocity is not inconsistent with TWA membership. This star was observed by

Mamajek *et al.*, but is not included in their final sample of candidate LCC Association members. Webb (W99) finds no Hα emission and an equivalent width of 0.17Åfor Li I 6708Å.

R4-42 AB Neither component in this late-type G-dwarf binary shows substantial chromospheric activity, and we exclude this system from TWA membership.

XACT 186 (also listed as c99a11 in W99) Another active K dwarf, the radial velocity is barely consistent with our predicted value, and we retain this star for further discussion.

HD 111265 A relatively weak X-ray source, this early-type G dwarf shows little evidence for chromospheric activity, and the apparent magnitude is consistent with a distance exceeding 100 parsecs. We therefore exclude this star as a possible TWA member.

CD -39 7118B The parallax listed in Table 2 is for the brighter star in this system. The level of chromospheric activity is relatively low for a 10-Myr-old K dwarf, although the rotational velocity is relatively high. There is significant lithium absorption (0.35Å equivalent width). This star may be a member of the LCC association, but it is unlikely to be a member of the nearer TWA cluster.

XACT 158 (also listed as c99b1 in W99) A late-type G dwarf, the coronal activity is consistent with an age comparable to that of the Pleiades. There is no evidence for Ca II emission and the Hα line is in absorption (W99). We regard this star as very unlikely to be a TWA member.

2M1139-31 One of the late-type M dwarfs identified as a possible TWA member by Gizis (2002) based on the presence of weak CaH and K I absorption, suggestive of low gravity. Gizis noted that the proper motion is inconsistent with other TWA members, and the level of chromospheric activity is consistent with Pleiades stars of the same spectral type. While this is likely to be a relatively young object, possibly a brown dwarf, it appears unlikely to be TWA member.

2M1207-39 The second M8 candidate member identified by Gizis has substantially higher Hα emission and proper motions consistent with other TWA members.

CD-40 7164 Catalogued as 7760-0836-1 by MF01, this late-type F dwarf has coronal activity consistent with Pleiades-age stars, although the lithium equivalent width measured by Song *et al.* (2002) suggests an age younger than IC 2602 (30 Myrs). On this basis, it is unlikely to be a TWA member, but we consider it further in the following section.

CD-49 7027 8238-1462-1 in MF01, the coronal activity and lithium equivalent width (Song *et al.*, 2002) lies near the upper extreme of the Pleiades sequence. Mamajek *et al.* identify the star as a member of the LCC association.

8234-2856-1 The third star from MF01, both the coronal and chromospheric activity levels lie nearer to 120-Myr Pleiades sequence than the known TW Hydrae members. The lithium equivalent width is consistent with data for IC 2602 stars (Song *et al.*, 2002). This is another star listed as a high-probability (86-98%) member of the LCC Association by Mamajek *et al.*.

As noted in §2.1, the last three stars are all identified as probable members of the LCC Association by Song *et al.*, with photometric distances estimated as 130 parsecs.

4. Space motions of the TW Hydrae Association stars

Radial velocities provide a one-dimensional test of whether candidate TWA members have kinematics consistent with cluster membership; full space motions provide a more stringent test, but require not only proper motion measurements but also reliable distance estimates. Proper motions are available for ten TWA members and for all of the surviving new candidates (Table 3). Distance measurements, in the form of Hipparcos parallaxes accurate to $\sim 10\%$, are available for only a handful of the brighter stars amongst the previously-known TWA members: TW Hydrae, at 56.5 parsecs; HD 98800 at 46.7 pc.; CD -36:7429 at 50.3 parsecs[2]; and HR 4796 at 67 parsecs. Figure 5 plots the (α, δ) distribution of the known TWA members and the candidates, flagging stars with independent distance estimates. The current TWA Association spans at least 40 degrees on the sky, corresponding to ~ 40 parsecs at the distance of TW Hydrae.

Given the observed distances and spatial extent of the known members, we have used two models to estimate distances,and hence space motions, for stars in Table 3 which lack parallax data. First, we assigne distances of 56 ± 15 parsecs; second, following the arguments outlined by ZWSB, we assume that the mean distance of the TW Hydrae association varies with position, and calculate individual distances using

$$d \ = \ 1.17\alpha \ - \ 137 \text{ parsecs}$$

[2]This system is a moderately-close binary, separation 6 arcseconds, but with a component flux ratio exceeding ten at blue/visual wavelengths, the Hipparcos astrometry should not be affected.

where α is Right Ascension, in degrees. This linear relation approximately matches the trigonometric distance to TW Hydrae, and places the association centroid approximately midway between HR 4796 and HD 102458 at the eastern extreme. These models allow at least a preliminary assessment of whether the space motions of the new candidates are likely to be consistent with cluster membership.

The resulting (U, V, W) velocities[3] are listed in Table 3 and plotted in Figure 6. In addition to the TW Hydrae stars, we plot data for CD-39 7118B, HD 102458 and the three MF01 Tycho stars, representing the space motion of the LCC Association, and we show the location of the Local Standard of Rest (LSR), using the Solar Motion derived by Dehnen & Binney (1998). The mean motion of the four TWA members with trigonometric parallax data is

$$(\langle U\rangle \;=\; -10.0 \pm 2.6;\; \langle V\rangle \;=\; -17.8 \pm 2.1;\; \langle W\rangle \;=\; -4.6 \pm 1.1\mathrm{km\ s}^{-1}$$

corresponding to a velocity of 13 km s^{-1} with respect to the LSR. The five background LCC stars have a similar mean motion,

$$(\langle U\rangle \;=\; -11.6 \pm 2.6;\; \langle V\rangle \;=\; -20.8 \pm 1.4;\; \langle W\rangle \;=\; -5.4 \pm 1.0\mathrm{km\ s}^{-1}$$

suggesting that the TW Hydrae Association is related to the larger LCC complex.

Both distance models produce a relatively elongated distribution of velocities for the known TWA members. The seven surviving new candidates lie on the boundaries of this distribution. One star, XACT 61, is well separated from all other stars in the latter diagram, and is therefore least likely to be associated with TW Hydrae. Of the remaining six stars, XACT 10 and HD 111265, are closest to the TWA grouping, under either distance model, and we conclude that the derived space motions do not exclude the possibility that they are members. On the other hand, assigning distances of 130 parsecs to all six stars (but not XACT 61) gives space motions consistent with the LCC system.

Considering the TWA members themselves, it is clear that current uncertainties in the distances, and hence space motions, preclude a reliable determination of whether all of the current TWA members originated in the same star-forming cloud. Yet the similarities in motion with respect to the LCC suggests that all are likely to have originated in that complex. Further observations, particularly trigonometric parallax measurements, are required to confirm or deny this hypothesis.

---

[3]U is positive toward the Galactic Centre, V is positive in the direction of Galactic rotation, and W is positive toward the North Galactic Pole.

5. Summary and conclusions

We have presented high-resolution spectroscopic observations of twenty stars in 16 systems which have been catalogued as members of the TW Hydrae association, and 16 stars identified as possible new members. Combining our observations with literature data for field and cluster stars, we have calibrated the range of coronal and chromospheric activity expected for such young stars as a function of spectral type. Based on that calibration, together with our radial velocity measurements, nine of the sixteen candidates can be excluded as possible new members of the TW Hydrae Association. We also suggest that the observed activity levels argue against membership for one of the M8 dwarfs identified as a possible TWA member by Gizis (2002) and for all three Tycho stars which survive Song *et al.*'s (2002) re-analysis of Makarov & Fabricius' (2001) proper motion study.

Five further stars are unlikely to be TWA members based on the (U, V, W) space motions deduced for an assumed distance of 56±15 parsecs. The remaining two stars, XACT 10 and HD 111265, have coronal/chromospheric properties and space motions which are not inconsistent with cluster membership, although further observations are required to verify this possibility. In the HR diagram, these stars lie between HR 4796 and the late-K and M dwarfs which comprise the bulk of the current sample. Even with the addition of our more accurate radial velocity measurements, however, it is clear that the current data do not have sufficient accuracy to determine whether all of the stars in the TW Hydrae Association formed within a single molecular cloud, or whether they have their origin in a more dispersed star-forming region. Accurate trigonometric parallax data, combined with a consistent set of reliable optical and near-infrared photometry, can go some way towards addressing this issue.

Thanks to Ben Zuckerman for originally promting these observations, and to Ben and Inseok Song for helpful comments on an earlier version of the paper. This research was supported partially by a grant under the NASA/NSF NStars initiative, administered by the Jet Propulsion Laboratory, Pasadena. We have made extensive use of the Simbad database, maintained by Strasbourg Observatory, and of the ADS bibliographic service.

REFERENCES

Bessell, M.S. 1979, PASP, 91, 589

de la Reza, R., Torres, C.A.O., Quast, G., Castillo, B.V., Viera, G.L. 1989, ApJ, 346, L61

Dehnen, W., Binney, J.J. 1998, MNRAS, 298, 387

Delfosse, X., Forveille, T., Perrier, C., Mayor, M. 1998, A& A, 331, 581

Ducati, J.R., Bevilacqua, C.M., Rembold, S.B., Ribeiro, D. 2001, ApJ, 558, 309

Fitzgerald, M.P. 1970, A&A, 4, 234

Flower, P.J., 1996, ApJ, 469, 355

Gliese, W., & Jahreiß, H. 1991, Preliminary Version of the Third Catalog of Nearby Stars, ADC/CDS Catalog V/70 (pCNS3)

Gizis, J.E., Monet, D.G., Reid, I.N., Kirkpatrick, J.D., Liebert, J. & Williams, R.J. 2000, AJ, 120, 1085

Gizis, J.E., 2002, AJ, in press (G02)

Gray, D.F. 1982, *The observation and analysis of stellar photospheres* Cambridge University Press, (New York, Cambridge)

Gregorio-Hetem, J., Lepine, J.R.D., Quast, G., Torres, C.A.O., de la Reza, R. 1992, AJ, 103, 549

Hawley, S.L., Gizis, J.E., & Reid, I.N. 1996, AJ, 112, 2799

Hawley S.L., Reid I.N., Gizis J.E. & Byrne P.B. 1999, "Chromospheric Activity in Low Mass Stars: Observational Results from Clusters and the Field", in *Solar and Stellar Activity: Similarities and Differences*, ed. C.J. Butler and J.G. Doyle, (ASP Conference Series No. 158), 63.

Herbig, G. H. 1978, Origin of the Solar System, 219

Huensch M., Schmitt J.H.M.M., Sterzik M.F., Voges W. 1999, A&AS, 135, 319

Jensen, E.L.N, Cohen, D.H., Neuhäuser, R. 1998, AJ, 116, 414

Jura, M., Malkan, M., White, R., Telesco, C., Pina, R., & Fisher, R. S. 1998, ApJ, 505, 897

Kastner, J.H., Zuckerman, B., Weintraub, D.A., Forveille, T. 1997, Science, 277, 67

Kraft, R.P., 1967, ApJ, 150, 551

Krist, J.E., Stapelfeldt, K.R., Ménard, F., Padgett, D.L., Burrows, C.J. 2000, ApJ, 538, 793

Makarov, V.V., Fabricius, C. 2001, A&A, 368, 866 (MF01)

Mamajek, E.E., Meyer, M.R., Liebert, J. 2002, ApJ, in press

Marcy, G.W., Benitz, K.J. 1989, ApJ, 344, 441

Micela, G., Sciortino, S., Harnden, F.R., Kashyap, V., Prosser, C.F., Damiani, F., Stauffer, J., Caillault, J.-P. 1999, A&A, 341, 751

Muzerolle, J., Calvet, N., Briceño, C., Hartmann, L., & Hillenbrand, L. 2000, ApJ, 535, L47

Parker, E.N. 1955, AJ, 122, 293

Reid, I.N., Gizis, J.E. 1997, AJ, 113, 2246

Reid, I.N., Hawley, S.L., Gizis, J.E. 1995a, AJ, 110, 1838

Reid, I.N., Hawley, S.L., Mateo, M. 1995b, MNRAS, 272, 828

Reid, I. N. & Mahoney, S. 2000, MNRAS, 316, 827

Reid, I.N., Kirkpatrick, J.D., Liebert, J., Gizis, J.E., Dahn, C.C., Monet, D.G. 2002b, AJ, in press

Skumanich, A. 1972, ApJ, 171, 565

Soderblom, R.R, Duncan, D.K., Johnson, D.R.H. 1991, ApJ, 375, 722

Song, I., Bessell, M.S., Zuckerman, B. 2002, A&A, 385, 862 (SBZ02)

Stauffer, J.R., Caillault, J.-P., Gagné, M., Prosser, C.F., Hartmann, l., 1994, ApJS, 91, 625

Stern, R.A., Zolcinski, M.-C., Antiochos, S.K., Underwood, J. 1981, ApJ, 249, 647

Sterzik, M.E., Alcala, J.M., Corvino, E., Petr, M.G. 1999, A&A, 346, L41 (SACP99)

Torres, G., Guenther, E.W., Marschall, L.A., Neuhauser, R., Latham, D.W., Stefanik, R.P. 2003, AJ, in press

Trilling, D.E., Koerner, D.W., Barnes, J.W., Ftaclas, C., Brown, R.H. 2001, ApJ, 552, L151

Ulmschneider, p. 1967, Zh. Ap., 67, 193

Urban, S.E., Corbin, T.E., Wycoff, G. L. 1998, AJ, 115, 2161

Vaiana, G. *et al.*, 1981, ApJ, 245, 163

Vogt, S.S. et al., 1994, S.P.I.E., 2198, 362.

Webb, R.A., 1999, Ph.d. thesis, University of California, Los Angeles (W99)

Webb, R.A., Zuckerman, B., Platais, I., Patience, J., White, R.J., Schwatrz, M.J., McCarthy, C. 1999, ApJ, 512, L63 (WZP99)

Weinberger, A.J., Becklin, E.E., Schneider, G., Chiang, E.I., Lowrance, P.J., Silverstone, M., Zuckerman, B., Hines, D.C., Smith, B.A. 2002, ApJ, 566, 409

Wilson, O.C., 1966, ApJ, 144, 695

Zuckerman, B., Reid, I.N. 1998, ApJ, 505, L143

Zuckerman, B., Webb, R.A., Schwartz, M., Becklin, E.E. 2001, ApJ, 549, L233 (ZWSB)

Table 1. TW Hydrae members and candidate members

TWA	Name	α 2000.0	δ	Sp. type	V	(B-V)	R	I	Ref.	(J)	H	K	Ref.	Source
	Members													
1	TW Hydrae^B	11 01 51.9	-34 42 17	K7	10.83	0.48	9.98	9.31	O1	8.46	7.65	7.37	I1	
2A	-29:8887A^B	11 09 14.0	-30 01 39	M0.5	11.60	2.21	10.25	9.20	O2, O3	7.85		7.18	I1	
2B	-29:8887B	11 09 14.2	-30 01 38	M2	13.50		12.40	10.70	O3	9.09		7.99	I1	
3A	Hen 600A^B	11 10 27.9	-37 31 53	M3	12.00		10.60	9.60	O2, O3	8.22	7.60	7.28	I1	
3B	Hen 600B	11 10 27.9	-37 31 52	M3.5	13.70		11.20	10.10	O3	8.63	8.07	7.80	I1	
4A	HD 98800Aab	11 22 05.3	-24 46 40	K5	9.41	1.11	8.40	7.50	O2, O3	6.44	5.82	5.65	I1	
4B	HD 98800Bab	11 22 05.3	-24 46 40	K5	9.94	1.40	8.80	7.40	O2, O3				I1	
5A	-33:7795A^B	11 31 55.4	-34 36 27	M1.5	11.72	1.72	10.40	9.10	O4, O3	7.71	7.06	6.83	I1	
5B	-33:7795B	11 31 55.4	-34 36 25	M8.5	20.40		18.10	15.80	O5, O6		12.1	11.5	I1	
6	^{B}	10 18 28.8	-31 50 02	K7	12.00	1.90	10.81	9.77	O5	8.79	8.17	7.97	I1	
7	^{B}	10 42 30.3	-33 40 17	M1	11.06	1.54	10.10	9.10	O5, O3	7.78	7.13	6.89	I1	
8A	^{B}	11 32 41.5	-26 51 55	M2	13.30		11.20	9.61	O5, O6	8.37	7.72	7.44	I1	
8B	^{B}	11 32 41.5	-26 52 08	M5			13.85	11.48	O5, O6	9.91	9.36	9.01	I1	
9A	-36:7429A ^{B}	11 48 24.2	-37 28 49	K5	11.32	1.65	10.63	9.60	O5	8.60	7.95	7.68	I1	
9B	-36:7429B ^{B}	11 48 24.0	-37 28 49	M1	14.10		12.98	11.45	O5, O6	10.06	9.41	9.14	I1	
10	^{B}	12 35 04.3	-41 36 39	M2.5	12.70		11.80	10.50	O7	9.17	8.55	8.19	I1	
11A	HR 4796A	12 36 01.0	-39 52 10	A0	5.78	0.01			O5, O3	5.80	5.80	5.80	I1	
11B	HR 4796B	12 36 01.2	-39 52 14	M2.5	12.80		11.80	10.60	O4, O	9.32	8.57	8.36	I1	
12	RXJ1121.1	11 21 05.6	-38 45 16	M2	13.60	1.50	12.60	11.35	O8					
13A	RXJ1121.3A	11 21 17.3	-34 46 46	M1	12.10	1.50	11.20	10.10	O8					
13B	RXJ1121.3B	11 21 17.3	-34 46 46	M2	12.40	1.50	11.20	10.10	O8					
14	^{B}	11 13 26.5	-45 23 43	M0	13.80		11.85	10.95	O4, O6	9.85				
15A	^{R}	12 34 20.7	-48 15 15	M1.5	14.10		13.51	11.94	O4, O6					
15B	^{R}	12 34 20.6	-48 15 20	M2	14.00		13.41	11.81	O4, O6					
16	^{R}	12 34 56.4	-45 38 07	M1.5	12.30		11.64	10.17	O4, O6					
17	^{R}	13 20 45.4	-46 11 38	K5	12.70		11.69	10.78	O4, O6					
18	^{R}	13 21 37.3	-44 21 53	M0.5	12.90		12.08	10.92	O4, O6					
19A	HD 102458A^B	11 47 24.6	-49 53 03	G5	9.10	0.70	8.75	8.40	O4, O3					
19B	HD 102458B^B	11 47 20.7	-49 53 04	K7	11.90		11.06	10.21	O4, O3					
20	A2-146^B	12 31 38.1	-45 58 59	M2	13.40		12.32	11.10	O9					W99
	Candidates													
	XACT 164 A^B	12 10 13.1	-48 55 27	G	10.70		10.50	10.25	O9					W99
	XACT 164 B^B	12 10 10.7	-48 55 48	K2	11.10		10.60	10.20	O9					W99
	XACT 164 C^B	12 10 9.5	-48 55 43	M2	15.30		14.00	13.00	O9					W99
	HD 110817^B	12 45 06.8	-47 42 58	K1	10.40	0.80	10.00	9.30	O10	8.70	8.23	8.10	I2	W99

Table 1—Continued

TWA	Name	α 2000.0	δ	Sp. type	V	(B-V)	R	I	Ref.	(J)	H	K	Ref.	Source
	HD 112227^B	12 48 07.8	-44 39 17	G8	9.70	0.72	9.30	8.90	O10	8.12	7.69	7.51	I2	W99
	HD 107434^B	12 21 9.6	-38 18 09	F6	8.10	0.48	7.85	7.60	O10					W99
	HD 114335^B	13 10 19.5	-32 48 20	F6	8.50	0.53	8.30	8.00	O10					W99
	XACT 10^B	9 47 19.9	-40 3 10	K1	10.97	0.76	10.55	10.10	O2, O3					W99
	XACT 61^B	10 32 43.9	-44 40 56	K2	9.75	0.96	9.15	8.60	O2, O3					W99
	XACT 136^B	11 35 03.8	-48 50 22	K1	10.35	0.75	9.90	9.50	O2, O3	9.22	8.93	8.86	I2	W99
	R 4-42AB W^B	11 54 09.6	-31 59 24	G8	7.30	0.75	7.00	6.70	O10					W99
	R 4-42AB E^B	11 54 11.0	-31 59 21	G8	7.50	0.75	7.20	6.90	O10					W99
	XACT 186^B	12 43 51.8	-39 46 16	K2	10.14	0.87	9.50	9.00	O2, O3					W99
	HD 111265^B	12 48 20.1	-42 37 34	G0	10.20	0.65	9.90	9.60	O2, O3					W99
	CD-39 7118B^R	11 27 28.8	-39 52 57	K2	10.20		9.60	9.10	O10					W99
	XACT 158^R	10 31 24.1	-14 33 36	G8	10.83	0.80	10.40	9.90	O9					W99
	2M1139-31	11 39 51.1	-31 59 21	M8	20.20		18.00	15.70	O7	12.67	11.99	11.49	I3	G02
	2M1207-39	12 7 33.4	-39 32 54	M8	20.50		18.30	16.00	O7	12.98	11.40	11.95	I3	G02
	CD-40 7164	12 13 07.0	-40 56 32	F8	9.80	0.51	9.55	9.25	O10					MF01
	CD-49 7027	12 21 55.7	-49 46 13	G7	10.00	0.77	9.60	9.25	O10	8.49	8.05	8.02	I2	MF01
	8324-2856-1	12 22 04.3	-48 41 25	K3	10.50	0.81	9.90	9.40	O10	8.78	8.27	8.17	I2	MF01

Note. — Column 1 gives the identifying number from WZP99 and ZWSB;
column 2 lists alternative designations, where XACT refers to optical identifications form the ACT Reference Catalog (Urban *et al.*, 1998) - the superscript ^{B} indicates that the star was observed with the blue HIRES configuration in the program described in this paper, ^{R} indicates observations with the red HIRES configuration;
columns 3 and 4 give the equinox J2000 positions;
Column 5 lists the spectral type, taken from WZP99 and ZWSB for known members, from W99 and SIMBAD for W99 candidates, and from G02 and SIMBAD for the remaining stars.
The final column lists the source for the new candidate members.
References for optical photometry:
O1 - Reid *et al.*(2001); O2 - V, B from Hipparcos catalogue (ESA, 1997); O3 - R, I estimated from V+sp. type ;
O4 - ZWSB; O5 - WZP99; O6 - V and/or R estimated from I+sp. type; O7 - optical colours estimated from JHK+sp. type;
O8 - R, I from SACP99, V from sp. type; O9 - Photometry derived from GSC2.2 + sp. type;
O10 - B/V from SIMBAD, R/I from sp. type.
References for infrared photometry:
I1 - WZP99; I2 - Mamajek *et al.* (2MASS); I3 - G02 (2MASS)

Table 2. Emission line strengths, activity and rotation

Name	Sp. type	$\pi \pm \sigma$	m_{bol}	Ca II K Å	Hβ Å	Hα Å	$\log \frac{f_\alpha}{f_{bol}}$	$\log \frac{f_X}{f_{bol}}$	vsin i km s^{-1}	v_{rad} km s^{-1}	$v_{pred.}$ km s^{-1}	References	Member?
Members													
TW Hydrae	K7	17.7±1.5	10.00	9.7	49.7	220.0	-1.58	-1.94	< 3	12.5	12.5	WZP99	Y
-29:8887A	M0.5	···	10.60	21.1	2.1	1.9	-3.51	-1.97	9	10.8	11.6	WZP99	Y
-29:8887B	M2	···	12.35	···	···	···	···	···	···				Y
Hen 600A	M3	···	10.10	28.1	10.1	21.8	-2.79	-2.25	3	13.4	12.1	WZP99	Y
Hen 600B	M3.5	···	10.60	···	···	7.1	-3.32	36:	···			WZP99	Y
HD 98800Aab	K5	21.4±2.3	8.85	···	···	0.0	···	-2.37	···	12.8	10.1	WZP99	Y
HD 98800Bab	K5	21.4±2.3	9.30	···	···	0.0	···	···	···				Y
-33:7795A	M1.5	···	10.00	23.0	5.7	13.4	-2.96	-1.93	> 30	9.5±5	10.5	WZP99	Y
-33:7795B	M8.5	···	5.55	···	···	···	···	···	···				Y
TWA 6	K7	···	10.25	20.8	2.4	4.7	-3.49	-2.18	55	16.9±5	15.0	WZP99	Y
TWA 7	M1	···	9.60	38.8	4.9	4.9	-3.44	-2.38	< 3	11.7	13.6	WZP99	Y
TWA 8A	M2	···	10.10	63.3	5.7	7.3	-3.51	-2.18	< 3	7.8	9.6	WZP99	Y
TWA 8B	M5	···	11.90	48.5	18.1	16.5	-3.49	···	5	7.8	9.1	WZP99	Y
-36:7429A	K5	19.9±2.4	10.15	15.3	0.6	2.3	-3.75	-2.15	7	10.6	9.7	WZP99	Y
-36:7429B	M1	19.9±2.4	12.00	14.1	5.3	5.0	-3.62	···	4	11.3	9.7	WZP99	Y
TWA 10	M2.5	···	11.00	45.0	3.6	8.4	-3.33	-2.25	< 3	6.6	7.2	WZP99	Y
HR 4796A	A0	14.9±0.8	5.60	···	···	···	···	···	···	6.3	6.9	WZP99	Y
HR 4796B	M2.5	14.9±0.8	11.10	···	···	···	···	-2.25	···			WZP99	Y
RXJ1121.1	M2	···	11.90	···	···	4.5	-3.56	-2.01	15:	10.9	11.6	SACP99	Y
RXJ1121.3A	M1	···	10.60	···	···	2.8	-3.72	-1.81	10	12.0	11.2±3	SACP99	Y
RXJ1121.3B	M2	···	10.60	···	···	4.0	-3.57	···	10			SACP99	Y
TWA 14	M0	···	11.45	···	···	8.2	-3.18	-2.07	···	16.0	12.4	ZWSB	Y
TWA 15A	M1.5	···	12.50	···	···	9.0	-3.38	-1.63	22	11.2	8.1	ZWSB	Y
TWA 15B	M2	···	12.35	···	···	10.5	-3.33	···	30			ZWSB	Y
TWA 16	M1.5	···	10.70	···	···	4.0	-3.70	-2.41	11	9.0	7.7	ZWSB	Y
TWA 17	K5	···	11.30	···	···	2.5	-3.69	-2.36	45	4.6±6	5.1	ZWSB	Y
TWA 18	M0.5	···	11.40	···	···	3.5	-3.66	-2.37	20	6.9±3	4.7	ZWSB	Y
HD 102458A	G5	9.6±1.4	9.00	1.3	abs	-0.6	···	-2.40	25	14.7±3	10.8	ZWSB	LCC?
HD 102458B	K7	9.6±1.4	10.70	16.6	1.3	2.8	-3.63	···	10	15.2		ZWSB	LCC?
TWA 20	M2	···	11.60	25.5	2.9	···	···	-2.26	30	8.1±4	7.9	W99	Y
Candidates													
XACT 164 A	G	···	10.00	abs	abs	···	···	···	< 3	34.9	9.5	W99	N
XACT 164 B	K2	···	10.80	7.6	3.3	abs	···	-2.30	50	22.5±5	9.5	W99	N
XACT 164 C	M2	···	13.50	11.7	3.7	7.1	-3.28	-1.22	< 3	13.9	9.5	W99	N?
HD 110817	K1	···	10.10	4.6	abs	0.4	-4.29	-2.33	10.0	10.9	7.4	W99	Y?

Table 2—Continued

Name	Sp. type	$\pi \pm \sigma$	m_{bol}	Ca II K Å	Hβ Å	Hα Å	$\log \frac{f_\alpha}{f_{bol}}$	$\log \frac{f_X}{f_{bol}}$	vsin i km s^{-1}	v_{rad} km s^{-1}	$v_{pred.}$ km s^{-1}	References	Member?
HD 112227	G8	···	9.60	4.0	abs	abs	···	-2.25	35.0	12.7±7	6.8	W99	?
HD 107434	F6	···	8.10	0.4	ans	···	···	···	< 3	-12.2	7.6	W99	N
HD 114335	F6	···	8.55	abs	abs	abs	···	···	< 3	10.1	3.4	W99	N
XACT 10	K1	···	10.70	3.4	abs	abs	···	-2.38	5	14.1	16.8	W99	Y?
XACT 61	K2	···	9.25	3.1	abs	abs	···	-2.72	15	10.6	14.6	W99	Y?
XACT 136	K1	···	10.10	1.4	abs	abs	···	-2.66	28	16.6±5	11.4	W99	?
R 4-42AB W	G8	···	7.15	1.1	abs	···	···	···	< 3	6.7	8.7	W99	N?
R 4-42AB E	G8	···	7.35	1.1	abs	···	···	···	< 3	7.7		W99	N?
XACT 186	K2	···	9.60	4.1	abs	abs	···	-2.56	5	11.0	6.3	W99	Y?
HD 111265	G0	···	10.10	abs	abs	abs	···	-3.69	< 3	6.3	6.5	W99	Y?
CD-39 7118B	K2	7.0±0.9	9.70	···	···	0.3	-4.46	-2.60	25	13.7±4	11.3	W99	N
XACT 158	G8	···	8.80	···	···	abs	···	-4.21	3	15.7	12.5	W99	N?
2M1139-31	M8	···	14.70	···	···	10.0	-4.25	···	···	9.7		G02	N?
2M1207-39	M8	···	15.00	···	···	300.0	-2.77	···	···	8.7		G02	Y?
CD-40 7164	F8	···	9.80	···	···	-0.8	···	-3.55	12	10.0	8.5	MF01, SBZ	LCC?
CD-49 7027	G7	···	9.90	···	···	-0.4	···	-3.85	18	12.0	8.9	MF01, SBZ	LCC?
8324-2856-1	K3	···	10.30	···	···	0.5	-4.07	-3.31	16	13.2	8.8	MF01, SBZ	LCC?

Note. — Column 1 gives the common name of each TWA Hydrae member or candidate member; column 2 lists the spectral type; column 3 lists Hipparcos trigonometric parallax data, if available; column 4 gives the apparent bolometric magnitude, derived from the photometric data listed in Table 1;
columns 5, 6 and 7 list the equivalent widths of emission at the Ca II K-line, Hβ and Hα - a value of 0.0 indicates no emission, (···) indicates that data are not currently available;
columns 8 and 9 list chromospheric activity, as measured by the ratio between the Hα flux and the bolometric flux, and coronal activity, the ratio between the X-ray flux measured by ROSAT and the bolometrix flux;
column 10 lists the rotational velocity - uncertainties are ± 3 km s^{-1} for $v \sin i < 25$ km s^{-1} , rising to ± 10 km s^{-1} for the fastest rotators. Rotational velocities for HD 98800Aab, RXJ1121.1, RXJ1121.3A and RXJ1121.3B are from Torres *et al.*(2003).;
column 11 the radial velocity, accurate to ± 2 km s^{-1} for $v \sin i < 15$ km s^{-1} - uncertainties are listed explicitly for fast rotators;
column 12 lists the predicted radial velocity (see §3.1);
column 13 lists the source of Hα measurements, radial velocities and rotational velocities for stars not observed in the course of our HIRES program;
finally, column 14 indicates whether the observed data are consistent with membership of the TW Hydrae association.

Table 3. Space motions

Name	V_{rad} km s^{-1}	μ_α mas.	μ_δ mas.	Ref.	d	U	V	W	Member?
TW Hydrae	12.5	-66.9	-12.4	1	56.4 ± 5.3	-12.0±1.6	-17.9±1.5	-5.0±1.5	
TWA 2AB	10.8	-90.8	-21.0	2	56 ± 15	-16.6±6.5	-19.3±2.5	-8.4±3.0	
					59 ± 15	-17.5±6.5	-19.8±2.5	-9.0±3.0	
TWA 3AB	13.4	-112.0	-11.0	2	56 ± 15	-21.8±7.5	-22.9±2.9	-8.7±5.5	
					59 ± 15	-23.1±7.5	-23.4±2.9	-9.4±5.5	
TWA 4ABab	12.8	-85.5	-33.4	1	46.7 ± 4.7	-11.3±2.1	-20.6±1.5	-4.8±1.6	
TWA 5AB	9.5	-82.0	-29.0	2	56 ± 15	-13.5±5.8	-19.0±2.5	-8.9±3.0	
					65 ± 15	-16.1±5.5	-20.8±2.5	-11.1±3.0	
TWA 6	16.8	-57.0	-21.0	2	56 ± 15	-9.3±4.0	-20.3±1.6	-6.5±3.1	
					44 ± 10	-7.4±2.5	-19.3±1.5	-3.8±2.5	
TWA 7	11.7	-122.0	-29.0	2	56 ± 15	-22.4±7.8	-21.4±2.4	-16.9±4.3	
					51 ± 10-20.3±5.5	-20.5±2.5	-15.0±3.5		
TWA 9AB	10.6	-54.1	-20.0	1	50.3 ± 6.0	-6.2±1.8	-15.9±1.4	-3.0±1.6	
TWA 10	6.6	-67.0	-43.0	2	56 ± 15	-9.4±4.7	-17.8±2.9	-9.2±3.8	
					84 ± 17	-15.7±6.0	-24.0±3.0	-15.0±5.5	
TWA 11AB	6.3	-55.9	-24.0	1	67.1 ± 4.7	-10.4±1.3	-16.6±1.5	-5.5±1.5	
HD 102458AB	14.9	-33.7	-10.2	1	104 ± 15	-7.4±2.5	-20.7±1.5	-5.8±1.5	LCC?
Candidates									
HD 110817	10.9	-30.3	-14.0	2	56 ± 15	-0.6±2.0	-14.0±1.3	-0.9±1.5	LCC
					87 ± 17	-4.0±2.5	-16.8±2.0	-3.0±1.5	
HD 112227	12.7	-34.4	-20.2	2	56 ± 15	-0.2±2.5	-16.5±1.6	-1.2±1.9	LCC
					88 ± 18	-4.0±3.0	-20.0±2.0	-4.0±2.8	
XACT 10	14.1	-43.7	20.1	3	56 ± 15	-12.6±2.8	-14.3±1.5	-0.6±2.7	Y?
					35 ± 8	-7.9±2.0	-14.1±1.5	0.6±2.0	
XACT 61	10.6	-97.7	59.7		56 ± 15	-28.4±6.2	-14.9±1.8	-2.6±4.7	N
					48 ± 10	-2.2±4.0	-14.3±1.5	2.5±3.0	
XACT 136	16.6	-24.7	-7.0		56 ± 15	0.6±2.0	-17.9±1.3	-0.1±1.6	LCC?
					66 ± 15	-0.3±2.0	-18.4±1.5	-0.8±2.0	
XACT 186	11.0	-31.0	-13.5		56 ± 15	-0.8±2.3	-14.2±1.8	-0.8±1.5	LCC?
					86 ± 17	-4.1±2.0	-17.2±3.0	-1.1±2.5	
HD 111265	6.3	-51.4	-13.9	2	56 ± 15	-7.5±3.3	-13.4±2.1	-1.4±1.5	Y?
					88 ± 18	-13.6±4.0	-18.2±2.5	-3.3±2.0	
CD-40 7164	10.0	-32.2	-12.2	2	130 ± 20	-11.0±4.5	-19.8±2.0	-6.1±3.0	LCC?
CD-49 7027	12.0	-38.9	-17.2	2	130 ± 20	-14.2±4.5	-22.8±2.5	-4.2±3.0	LCC?
8324-2856-1	13.2	-32.4	-8.1	2	130 ± 20	-11.6±4.5	-19.2±2.5	-4.5±1.5	LCC?

Note. — Column 1 lists the TWA identification or common name; Column 2 lists the radial velocity; Columns 3 and 4 give the proper motion, in milliarcseconds; Column 5 lists the source of the astrometry: 1. Hipparcos (ESA, 1997); 2 - Tycho ; 3 - Web (1999); 4 - Gizis (2002)
Columns 6,7 and 8 list the derived (U, V, W) space motions, where U is positive toward the Galactic Centre; V, positive in the direction of rotation; and W positive toward the North Galactic Pole. The uncertainties, ϵ, are derived from undertainties in proper motion, radial velocity and distance, setting $\epsilon = 1.4$km s^{-1} as a lower limit.

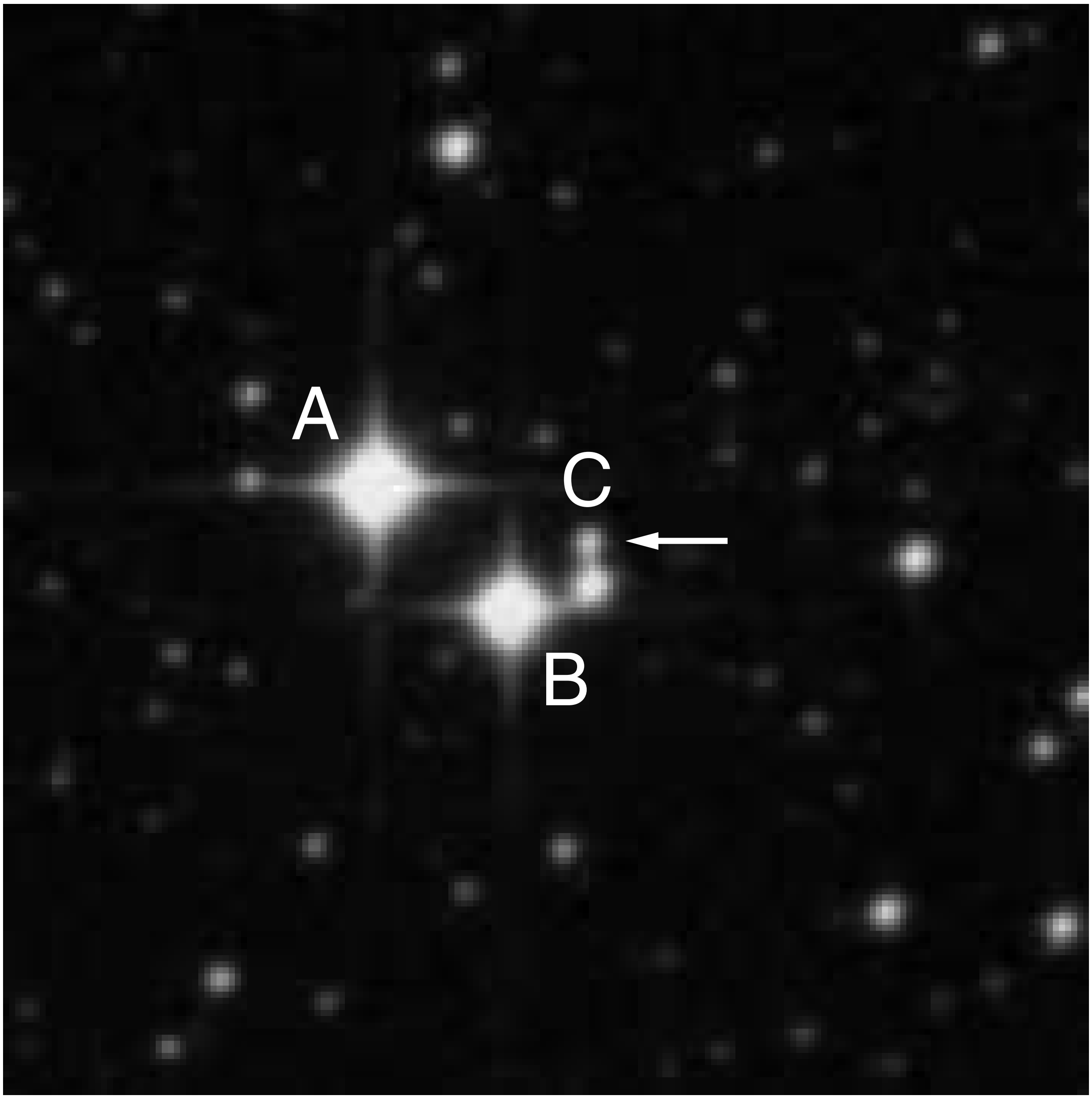

Fig. 1.— The 4×4 arcminute region centred on the position of XACT 164 (from the POSS II F-plate in the Digitised Sky Survey). The three candidate optical counterparts are identified and discussed in the text.

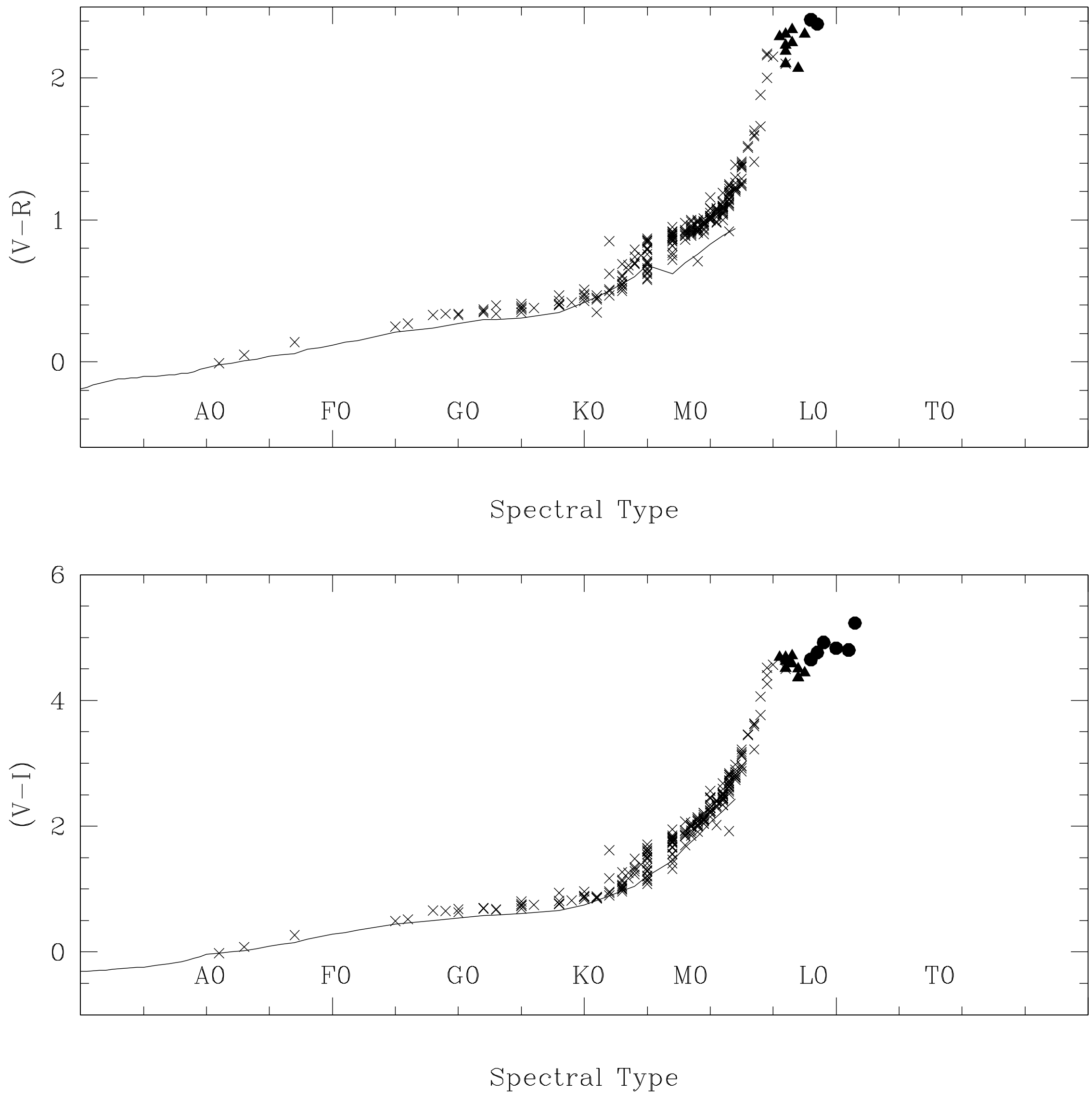

Fig. 2.— (V-R) and (V-I) colours as a function of spectral type: lines plot the transformed mean relations from Ducati *et al.*(2001); the symbols plot data for stars within 8-parsecs (crosses), ultracool M dwarfs (triangles) and L dwarfs (solid points). Note that the spectral sequence runs ..K4, K5, K7, M0... We adopt the median colour derived from the observed datapoints in estimating magnitudes for the TWA candidates.

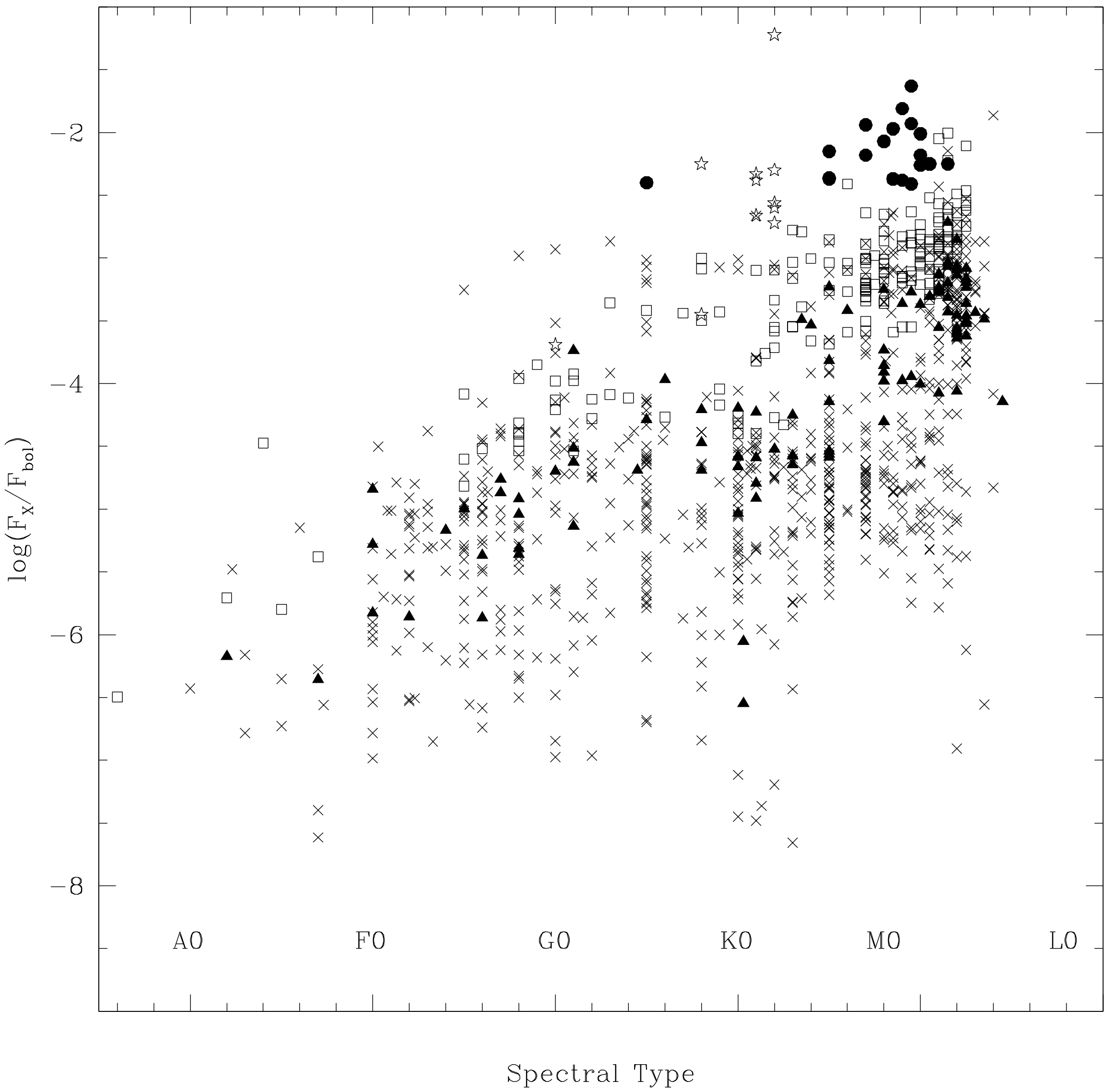

Fig. 3.— Coronal activity as a function of spectral type. The crosses mark data for field stars in the immediate Solar Neighbourhood (from Huensch *et al.*, 1999); solid trinagles are data for the Hyades cluster (Reid *et al.*, 1995a; Stern *et al.*, 1981); open squares are data for the Pleiades (Stauffer *et al.*, 1994; Micela *et al.*, 1999). Solid points mark data for TWA members; 5-point stars plot data for the candidates listed in Table 1.

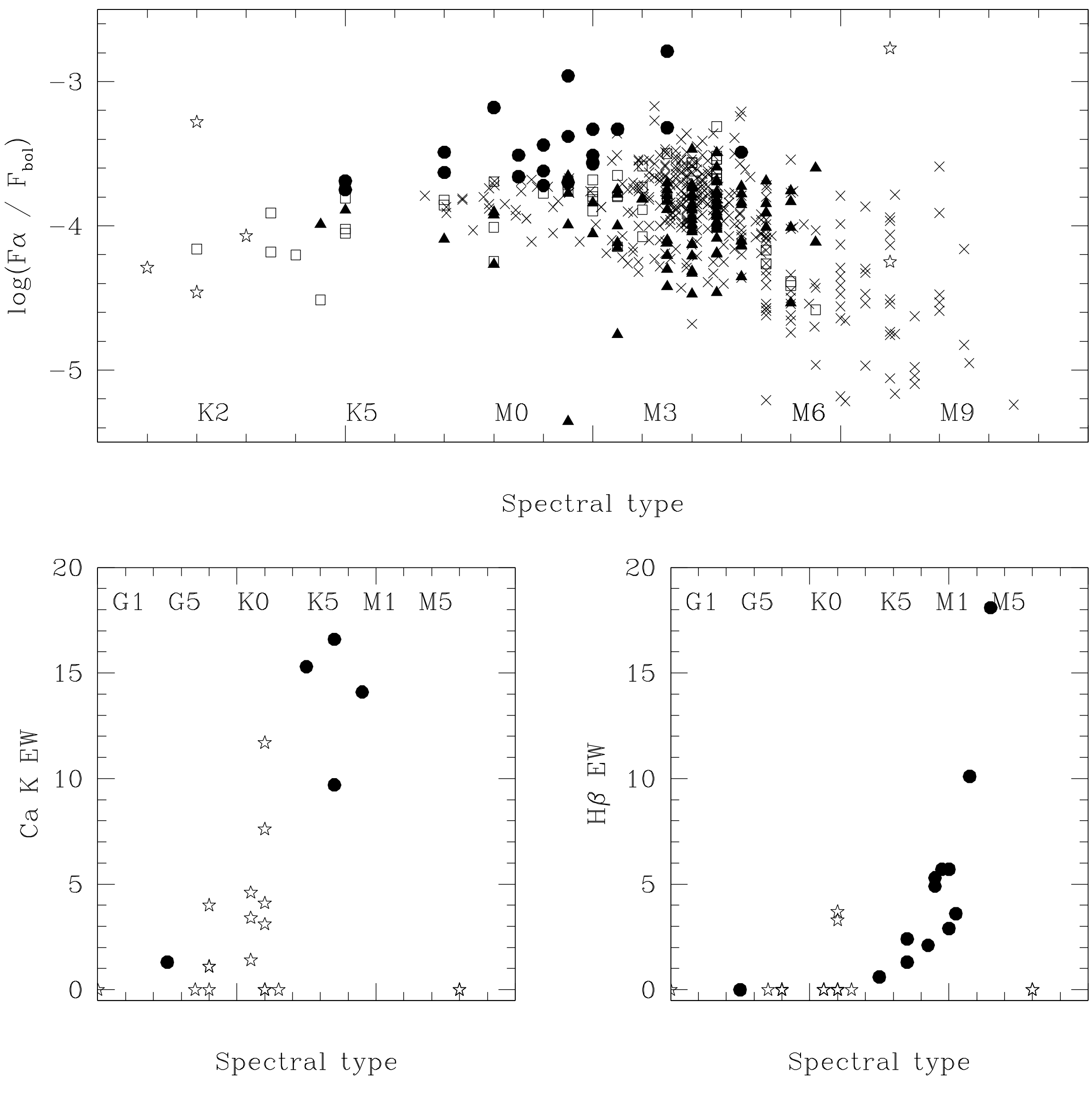

Fig. 4.— Emission line activity of the TW Hyadrae candidate members. The upper panel plots Hα activity as a function of spectral type, with the symbols having the same meaning as in Figure 8. The offset between earlier-type Hyades and Pleiades stars is less pronounced at Hα than at X-rays since most of the Hyades stars with emission are binaries. The lower two panels compare the Ca K and Hβ emission line widths of the new candidates against data for previously identified members.

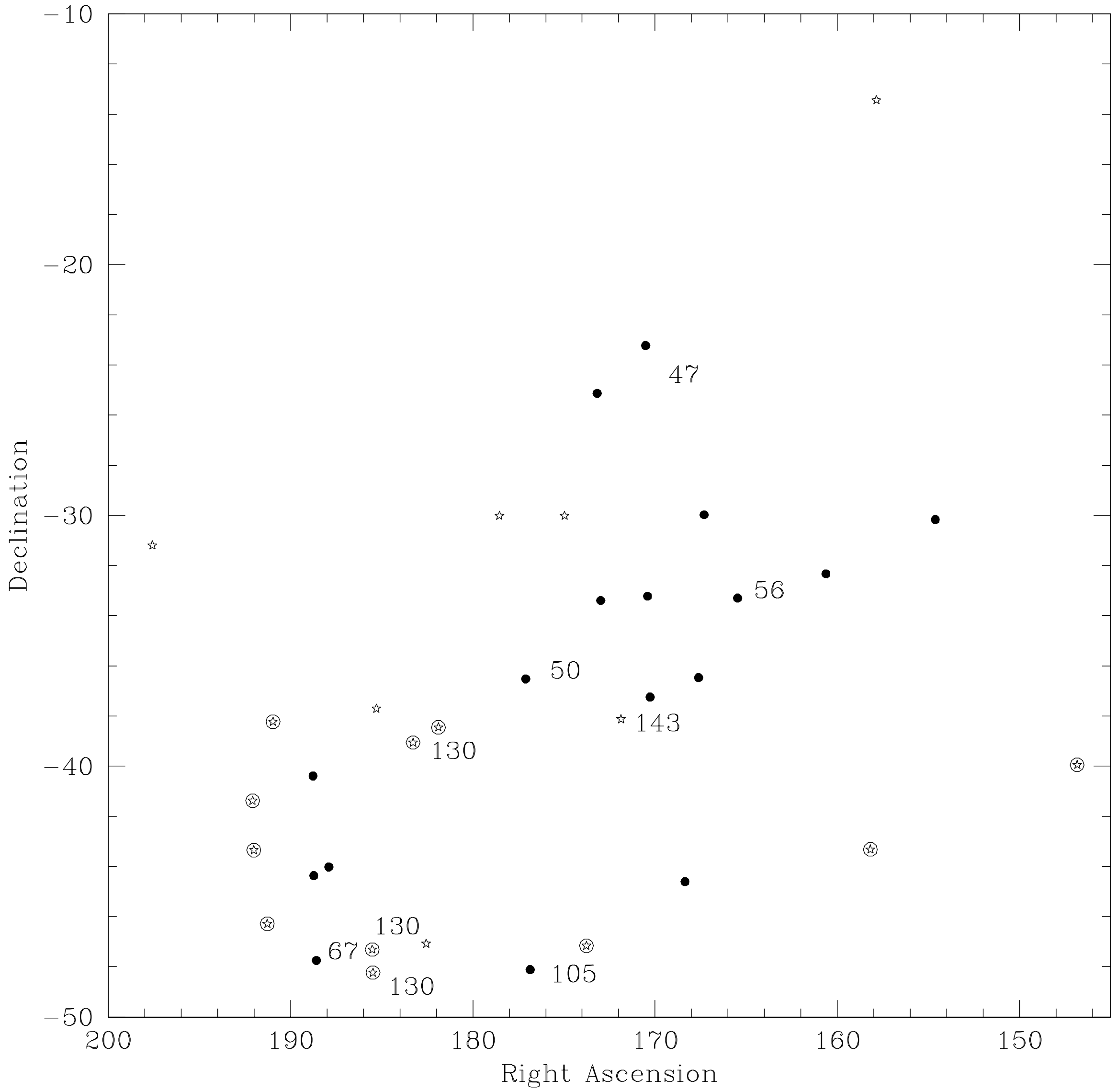

Fig. 5.— The (α, δ) distribution of known TW Hydrae members (solid points) and candidate members (five-point stars). The subset of the latter stars listed in Table 3 are enclosed in circles. The numbers list distance estimates for stars with independent distance estimates.

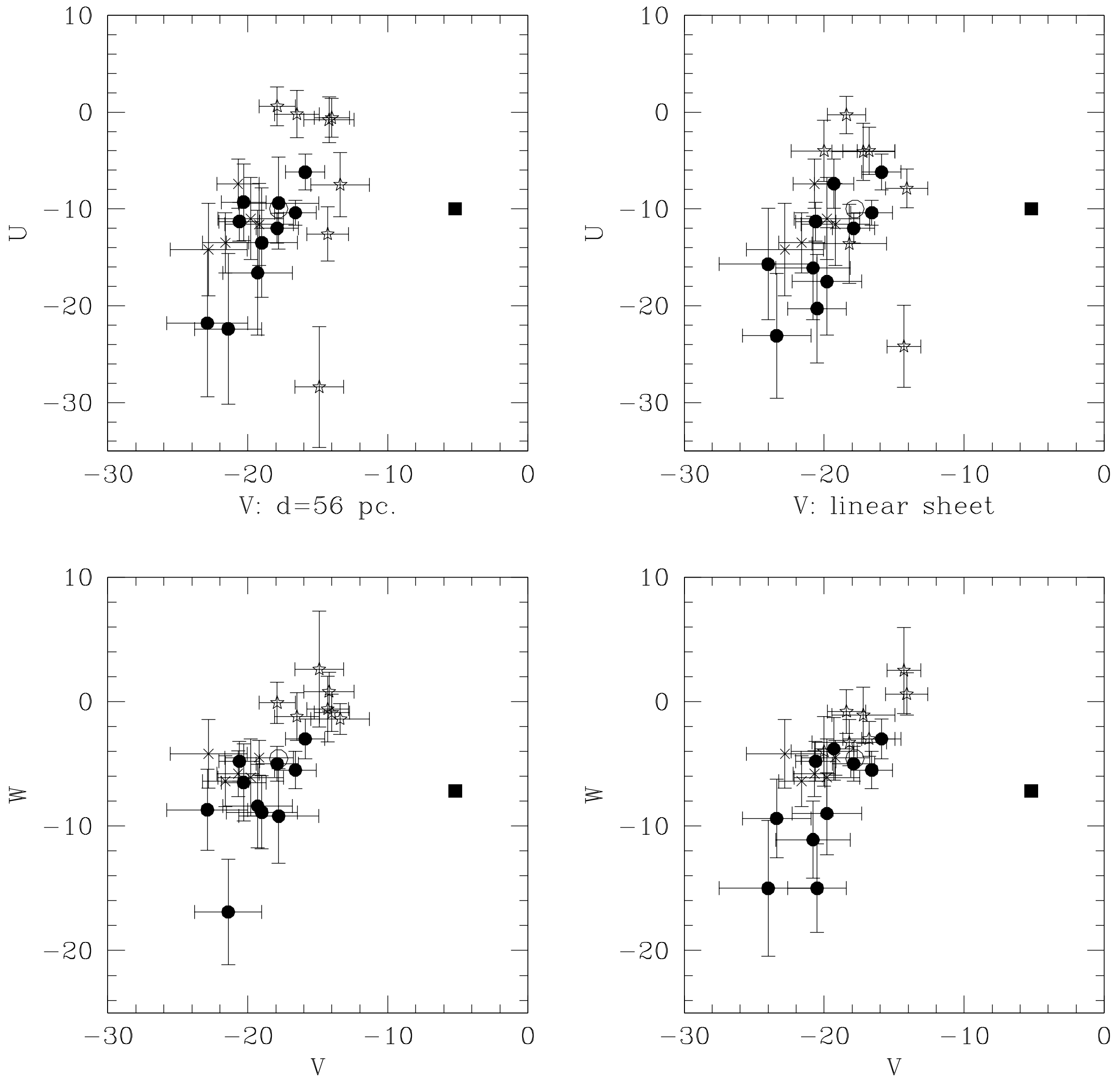

Fig. 6.— The (U, V, W) space motions of known TWA members (solid points) and new candidates (5-point stars), including only stars with both proper motion and radial velocity measurements (see Table 3). The left-hand panels plot the results if we assume d=56 ± 15 parsecs for stars lacking parallax data; the right-hand panels plot results is we assume the linear distance gradient described in the text. In both cases, the three MF01 stars, CD-39 7118B and HD 102458, representing the LCC Association, are plotted as crosses. The open circle marks the mean velocity of the TWA members with measured trigonometric parallaxes, and the solid square identifies the location of the Local Standard of Rest.